Photogrammetric Week '13 Dieter Fritsch (Ed.) Wichmann/VDE Verlag, Belin & Offenbach, 2013



# Oblique Image Data Processing – Potential, Experiences and Recommendations

DIETER FRITSCH, MATHIAS ROTHERMEL, Stuttgart


## ABSTRACT

Since about 10 years photogrammetric image data collection provides digital data of outstanding quality and high resolution. Digital camera technology is offering astonishing improvements – this trend will most probably be maintained in the next years to come. The "pixel race" for airborne image sensor systems behaves quite similar as the low-cost, off-the-shelve consumer camera market.

Dense Image Matching (DIM) has undergone a renaissance with the invention of Semi-Global matching. The resulting point clouds are superior in density and geometric accuracy, in particular for 80% forward and 80% cross overlaps. This demands for a discussion about the current NMCA country-wide flight patterns, which are quite often flown at 75-80% forward and 30% cross overlaps. Oblique airborne camera systems complement the birds-eye views and deliver point clouds for vegetation, building facades and other features to be used for comprehensive landscape and 3D city modeling.

Integrated solutions in photogrammetry are therefore still on the agenda, even if huge progress has been made. Remember the integration of DGPS/GNSS and IMU observations to directly deliver the parameters of exterior orientations, no matter if an image sensor or laser scanner has to be positioned and oriented. With the availablility of nadir and oblique imagery a new challenge for integrated solutions at point cloud level has to be overcome. This paper will therefore give some examples and thoughts how to solve this problem.


## 1. INTRODUCTION

The further developments of Dense Image Matching (DIM) algorithms, triggered by the introduction of the Semi Global Matching (SGM) method (Hirschmueller, 2005), offer new potential for aerial photography. National Mapping and Cadastral Agencies (NMCAs) fly countrywide aerial data collections with Ground Sampling Distances (GSD) of 10cm or even less. The resulting 3D point clouds could therefore easily cover about 100 points per sqm. Due to geometrical constraints embedded in the DIM process these point clouds are of superior geometric quality – are covering roofs, streets and vegetation with noise levels of less than 0.3GSD (Fritsch et al., 2013). The information content of a colored urban point cloud of GSD@10cm is very impressive and demands for new ideas and follow-up processing (see figure 1).

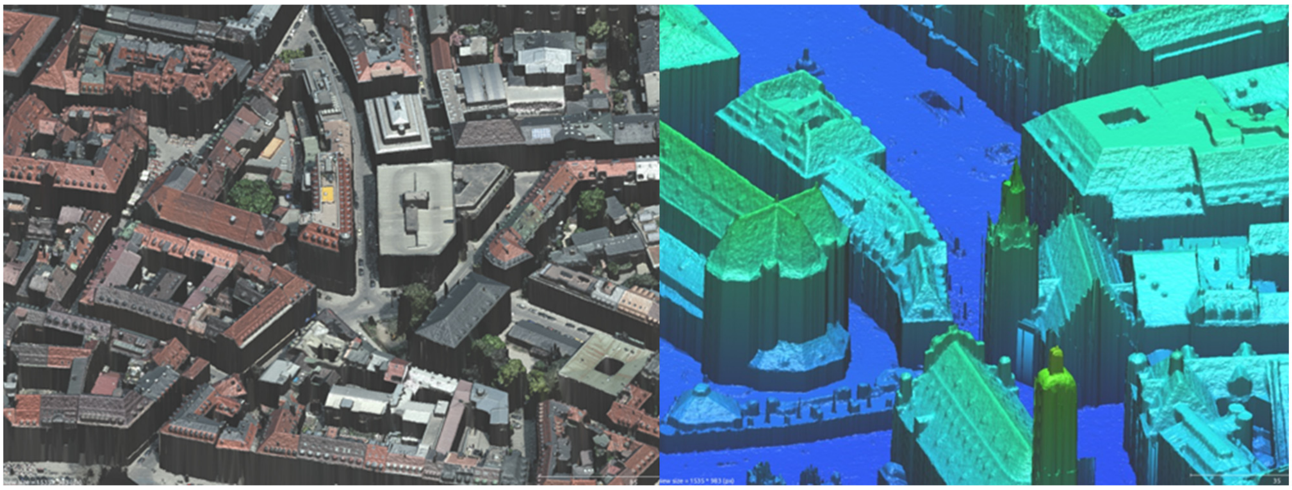

Figure 1: Munich colored point cloud (left), and point cloud with fine details (right), processed with SURE@ifp.

This offers more potential for information extraction using aerial photography, which has led to definition of "All-In-One Photogrammetry" (Fritsch et al., 2012), to provide besides 3D point clouds, the Digital Surface Model (DSM) and true orthophotos also 3D roof structures and corresponding 3D building models needed for updating 3D urban databases.

First experiments with the Hessigheim point clouds (collected by IGI DigiCAM@50MP, Fritsch et al., 2013) have shown the potential just by using simple image processing algorithms. DIM delivers a very dense 3D point cloud (figure 2 upper left&right), which can be filtered to differentiate between building features and vegetation by an opening operator of mathematical morphology – a DTM is obtained. Unregistered buildings are detected in the dDSM for those areas higher than a threshold@3m and are not registered in the ALKIS database (figure 2 lower left). Finally one undetected building block has been manually erected using Trimble's SketchUp software (figure 2, lower right).

Figure 2: Hessigheim colored point clouds (upper left), grey-shaded point cloud (upper right), unregistered buildings (lower left), and manually reconstructed 3D CSG building model (lower right).

To go along with the information content hidden in aerial photography necessitates for an update of methodology for semi-automatic and automatic 3D CSG building modeling, which has used in the past quite often the footprints of the buildings to be erected and intersected with automatically extracted 3D roof elements (Brenner, 2001, Kada, 2009). This is in contrary to the task to detect and reconstruct unregistered buildings in urban databases, as demanded by NMCAs and further public institutions.

With the evolution in airborne photography to complement nadir imagery with oblique views the missing building information along the building facades is made available. Therefore, some new oblique airborne camera systems are commented in chapter 2. The processing of this combined airborne photography is tested in two different scenarios, described in detail by chapter 3. Chapter 4 gives some recommendations for flight patterns, camera calibration and point cloud processing. The paper is concluded by a summary, acknowledgements and the references.

## 2. COMBINATION OF NADIR AND OBLIQUE IMAGERY

Digital oblique airborne imaging sensors seem to be successful complements of nadir-looking camera geometry. Those systems are useful for high accuracy 3D urban mapping and 3D corridor mapping applications. They are based on multiple camera arrangements (MultiViews), featuring up to 5 single cameras (PentaView) with different viewing directions. The history of framed oblique aerial photography goes back to the 1930s (Halley, 1938, Petrie, 2009), when first film-based oblique aerial images have been collected for mapping applications by the Fairchild T-3A system (figure 3).

With the development of digital pushbroom camera systems, the idea of combining nadir and oblique views became obvious and could be realized. Originally invented by the pioneer Otto Hofmann, already in the late 1970s, the first operational spaceborne system of this kind was the MOMS02 sensor – it combined a high resolution nadir CCD array with low resolution forward and backward looking CCD lines. Four nadir-mode multispectral image lines (RGB-IR complemented its pan imagery.  As a follow-up of this development the first operational airborne system was the Digital Photogrammetric Assembly (DPA), for which an extensive assessment test was launched 1995 by the Institute for Photogrammetry, University of Stuttgart in cooperation with the Agency for Military Mapping Services, Euskirchen/Germany (Fritsch, 1997). Nowadays, the high-end push-broom sensor systems, e.g. the ADS100 system of Hexagon/Leica Geosystems, follows the tradition of this successful imaging concept.

Digital oblique frame camera systems became most popular by the image datasets collected by Pictometry International, when the delivery of high resolution oblique imagery started in 2000. Their system is similar to the "Maltese Cross" pattern of the Fairchild T-3A (figure 3 center&right). Originally aiming at emergency documentations a boost of their image datasets could happen due to the launch of virtual globes such as Google Earth and MS Bing Maps 3D, to name just the two most popular ones. Very soon the potential for 3D city modeling and 3D building database update became feasible (Karbo&Schroth, 2009).

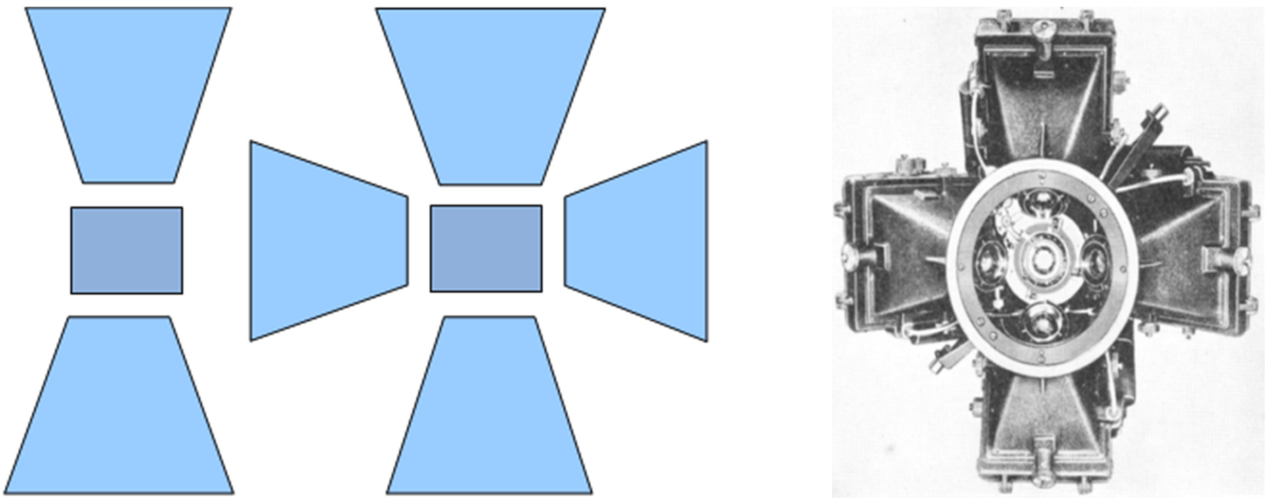

Figure 3: TrioView: 2fold oblique, 1 nadir (left), PentaView: 4fold oblique, 1 nadir (center), Fairchild T-3A System (1934) (right).

Nowadays several vendors offer digital oblique airborne camera systems – some of them are presented during this year's Photogrammetric Week. Leica Geosystems, a subdivision of Hexagon, features the new RCD30 Oblique, a 60 MP multispectral medium format camera which consists of one nadir and four oblique viewing cameras (PentaView). The system can easily be upgraded to 80MP and has a multi-directional motion compensation on-board, to deliver the highest image quality (figure 4 left, Wagner, 2013). IGI is featuring the *Penta DigiCAM,* which is based on five *DigiCAM* modules – four of them are looking in oblique and one in nadir direction (PentaView). All five cameras are handled as one system or individually. The system is best for quick data collections of nadir and oblique imagery within one flight. Its user interface is bundled in one screen. All GNSS/IMU and camera control units are fixed to one unit and can be mounted on top of the camera (figure 4 center). Another new system is the MS UltraCam Osprey, presented for the first time at the ASPRS 2013 Conference, Baltimore. This camera system combines a nadir panchromatic high-resolution image, one true-color RGB image, one NIR image and 6 oblique true-color images taken at an off-nadir angle of 45°. The system features dual oblique cones forwards and backwards, and single cones left and right and represents therefore also a PentaView system.

Figure 4: Three PentaView frame-based digital airborne camera systems: the Leica RCD30 Oblique (left), the IGI Penta DigiCAM (center) and the Microsoft UltraCam Osprey system (right).

A somewhat different architecture has been designed and built by VisionMap, Tel Aviv. Their A3 camera system is following the stepping frame sampling concept. A sequence of oblique aerial photos is exposed cross-track at a very high speed and with large focal length (e.g. 300mm) to provide a very wide angular coverage of the ground (figure 5 left). The system features a dual lens metric camera, has a folded optics, and may cover a maximal sweep angle up to 104° (figure 5 right). The imagery is stabilized with FMC and SMC – the large focal length requires a mirror-based optical compensation. The cross-overlap between two sweeps can be controlled and may reach close to 60%.

A comprehensive test for the A3 camera geometry was carried out in a close cooperation between VisionMap and the Institute for Photogrammetry, University of Stuttgart, using the Vaihingen/Enz testsite in June 2009). The evolution and processing chain of this camera system is given by Raizman (2013).

VisionMap requested as well a detailed ifp study on DIM, which is presented as a brief excerpt in chapter 3.3. For this test a special arrangement of the A3 system has been flown to deliver good coverage of an urban area to be investigated.

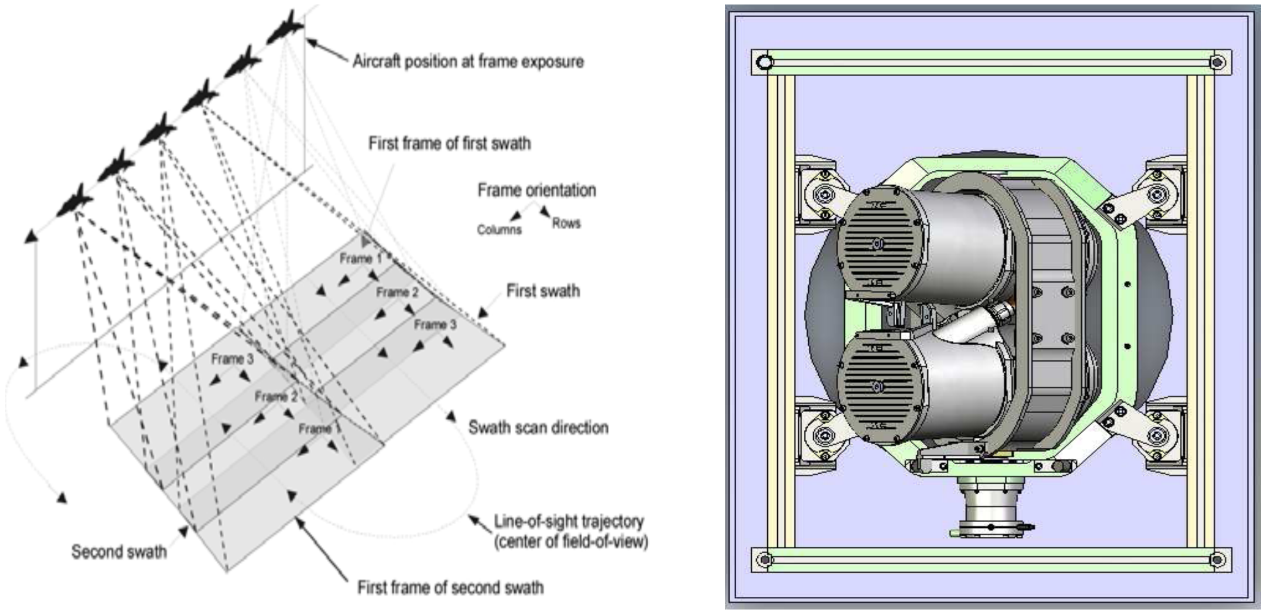


Figure 5: The stepping frame concept (left) – a CAD model of the A3 camera system (right).

## 3. DENSE IMAGE MATCHING USING OBLIQUE IMAGERY

The Institute for Photogrammetry has carried out extensive research in the area of DIM for the last four years. Some very challenging projects had to deliver dense 3D point clouds, no matter for which kind of imagery: airborne and close range, nadir and oblique. Thanks to our cooperation partners who trusted the ifp competence all the time. The outcome of this work is a piece of software called SURE – SUrface REconstruction using Images (Rothermel et al., 2012, Wenzel et al., 2013). This software is offering binary files free for academia – for those who would do some commercial projects can get licenses.

### 3.1. Oblique Imagery – Opportunities and Challenges

Once the nadir and oblique imagery is oriented DIM methods provide 3D point clouds providing substantially increased completeness in comparison to nadir-only datasets. Due to the additional oblique views façade points can be extracted. This is specifically suitable for the automatic derivation of 3D building models. The challenges for the processing of oblique imagery are the varying image scales and the low similarity due to wide baseline configurations and resultant changes in the perspective. Thus, combining aerial nadir and oblique imagery is quite similar to the situation in close range applications to reconstruct complex objects from imagery possessing large changes in viewpoints. The original idea of SGM uses a global smoothness constraint to compute a low noise parallax or disparity for each pixel even for low textured surfaces. Therefore, a constant disparity search space is normally used suitable for nadir image configurations. Being aware of the terrain undulation this range can easily be estimated. With oblique imagery the disparity search space increases significantly, causing an increase in processing time and memory requirements. SURE overcomes this problem by employing a modified SGM method which is called tSGM – tube-based SGM. Using several resolution levels the search space is derived for every pixel individually, reducing not only computing costs but also resolving matching ambiguities.

### 3.2. Assessment Test of the IGI Quattro DigiCAM Family

A first comprehensive test for the combination of nadir and oblique imagery has been carried out by the Institute for Photogrammetry, Univ. Stuttgart in cooperation with IGI mbH, Kreuztal/Germany to assess the performance of the *Quattro DigiCAM* (figure 6 left) in combination with the *Quattro DigiCAM Oblique* (figure 6 right), the predecessor of the *Penta DigiCAM*. The *Quattro DigiCAM* system collects four nadir images in a two by two pattern with small overlap. As the images are taken synchronously and with the same camera settings they can be stitched together geometrically and radiometrically to deliver one large format image. For the *Quattro DigiCAM Oblique* configuration the camera modules are mounted to point forward, back, left and right with an oblique angle of 45°.

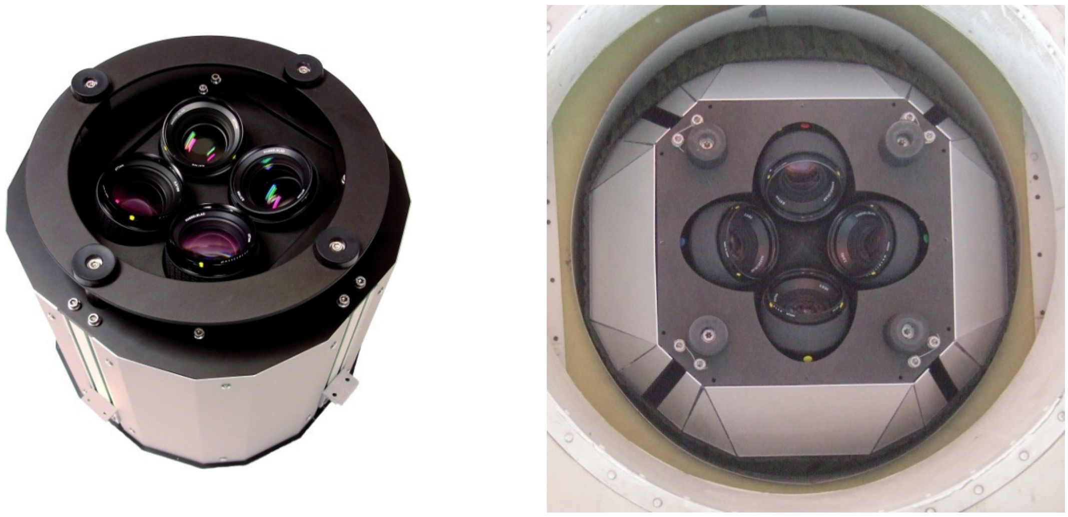

Figure 6: The IGI Quattro DigiCAM Family – left: Quattro DigiCAM, right: Quattro DigiCAM Oblique.

During data collection the same time stamp from the integrated *AEROcontrol GNSS/IMU* system can be used to obtain the exterior orientation parameters for each single camera at the same point in time. To ensure an optimal match between the nadir and oblique images, an *Integrated Sensor Orientation (ISO)* has been performed. For the measurement of the tie points MATCH-AT from Trimble was used – the final bundle block adjustment have been performed with BINGO from GIP, Aalen/Germany.

AEROWEST GmbH, Dortmund/Germany provided the image data, which were flown over the area of Luenen/Germany. As the nadir images could be collected on March 4th, 2011, there was a delay of about two month to collect the oblique imagery on May 5th, 2011. The nadir image block contained 917 large format virtual images with 60% forward and 50% cross overlap. A Ground Sampling Distance (GSD) of 10cm could be resolved, from a flying height of 830m. This dataset was complemented by 757 oblique images for each of the four cameras, with a GSD ranging from 6.7cm to 13.6cm, collected from a flying height of 760m. For the assessment test a sub block consisting of 48 nadir images (in four strips) and 170 oblique images have been selected (Figure 7).

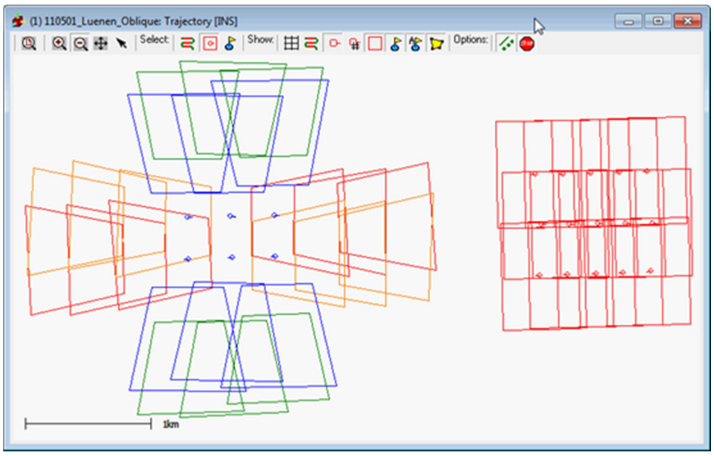


Figure 7: Example of the image footprints (only a few images are shown).

### 3.2.1. Point Cloud Generation Using IGI Quattro DigiCAM

The evaluated oblique dataset provides 66% forward overlap. Due to changes in perspective, variances in image content are rather large in contrast to a similar nadir configuration. Within the processing one master image is selected. For the point cloud generation its two neighboring images (slaves) from the same flight strip are selected. Moreover, overlapping images from neighboring flight strips are incorporated into the matching process. Therefore only image pairs providing an overlap of more than 20% are considered. The main challenge for matching these image pairs is the change of image content due to the largely differing image scale. For the present oblique dataset this leads to image configurations as exemplary shown in figure 8. It has to be clarified that only views possessing the same line of sight were incorporated into the matching process. Thereby the overlap of all processed models amounts at least 20% and angles between the view directions are smaller than 30 degrees. Within the processing all selected images are matched against the master image. For each stereo pair dense disparity maps are computed. Redundant information contained by the multiple models is later fused within the triangulation step. Note that only oblique imagery was used to generate the point clouds.

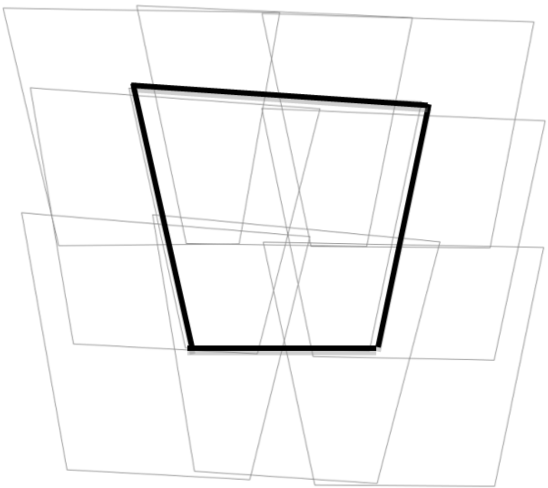

Figure 8: Exemplary matching configuration. The bold black frame marks the footprint of the master image, thin frames mark the footprints of the matched slave images.

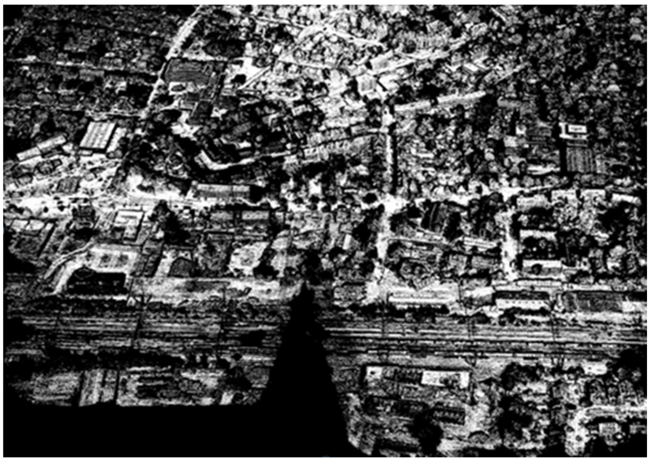

Figure 9: Successfully matched and triangulated points for an exemplary base image (encoded white). Black areas mark regions where matching or the consistency check within the triangulation process failed.

Processing overlapping imagery results in measurements of the same object point in multiple stereo models. As described in [Rothermel at al., 2012] this redundancy can be used to efficiently eliminate outliers and to increase the accuracy of the generated point clouds. An efficient method for detecting and eliminating mismatches was implemented for the processing of oblique imagery. Thereby, measurements of single stereo models and their matching uncertainty are transferred into object space and checked for consistency. Only if a certain number of measurements are consistent, they are assumed to be correctly matched and used for triangulation. The actual triangulation problem is nonlinear. Within SURE it is reduced to a one-dimensional optimization problem which is solved using an iterative Gauss-Newton process. Figure 9 encodes consistent and successfully triangulated object points from stereo models for an exemplary base image and six match images. Matching and triangulation of each base image results in one point cloud. All generated point clouds are eventually merged in object space.

### 3.2.2. Resulting Point Clouds Using IGI Quattro DigiCAM

The implemented matching strategy results in extremely dense surface models providing good accuracy and completeness. For a 570x630m large test area approximately 105 million points were extracted. The point density might be sufficient for the generation of true orthophotos (figure 12 and 13). Figure 11 displays the average matching success rates for the matching configurations displayed in figure 10. As expected due to the higher similarity of image content the number of successfully matched pixels in image pairs from the same flight strip is slightly larger. Nevertheless, also cross strip stereo pairs can be successfully matched even though same ground areas have different image scale. Note that the density is reduced within the subsequent consistency check in the triangulation process.
In contrast to nadir imagery for which typically only 2.5D models can be generated, for the present oblique data set dense 3D reconstructions can be obtained. Beside house facades also small 3D structures as for example balconies or cars (figure 14) can be extracted providing good precision. Even objects which are difficult to match, as solar panels or vegetation, are reconstructed due to high the redundancy. As typical for the Semi Global Matching algorithm abrupt steps in depth are maintained and distinct borders lines can be reconstructed reliably.

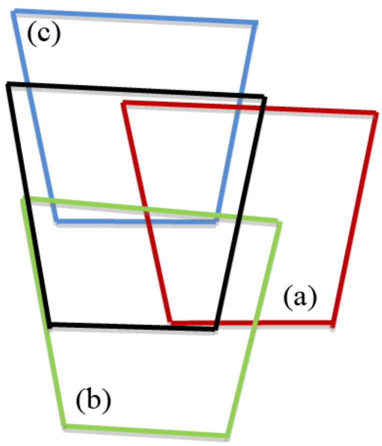


Figure 10: Master and slave image matching configurations; the black frame marks the master image, red frame (a) marks the in-strip matched slave image, green and blue frames (b) & (c) mark cross-strip matched slave images.

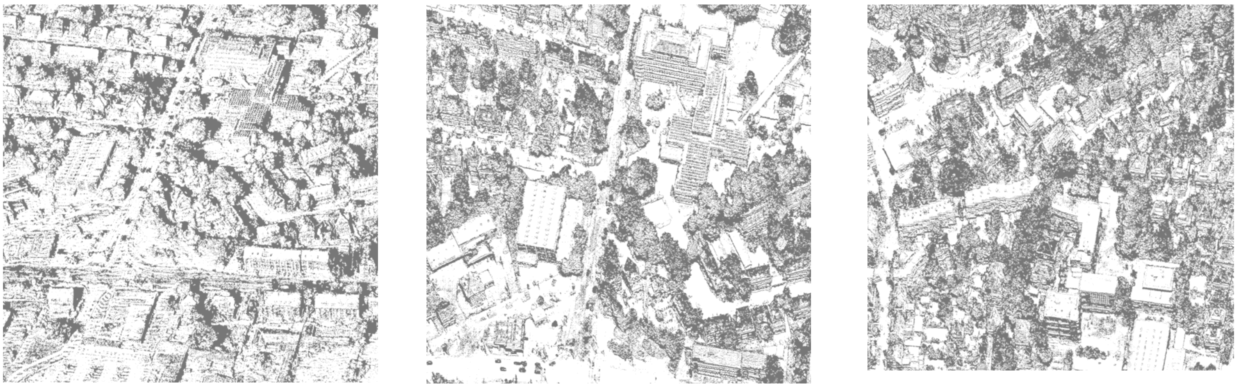

64.5% matched pixels 59.9% matched pixels (c) 53.4% matched pixels

Figure 11: Images encode successfully matched points (white), in grey areas matching failed

Figure 12: Ortho view of reconstructed point cloud (original colors).

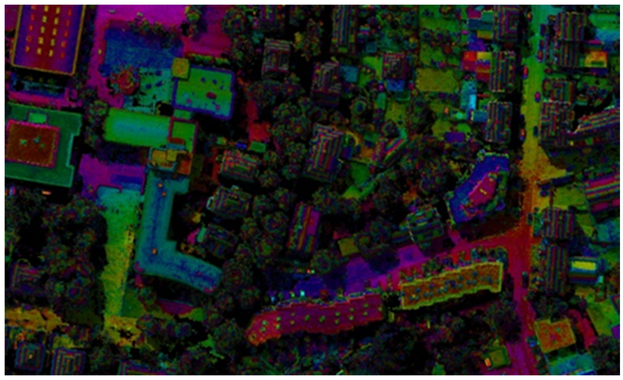

Figure 13: Ortho view of reconstructed point cloud (height decoded, one color cycle equals 2m).

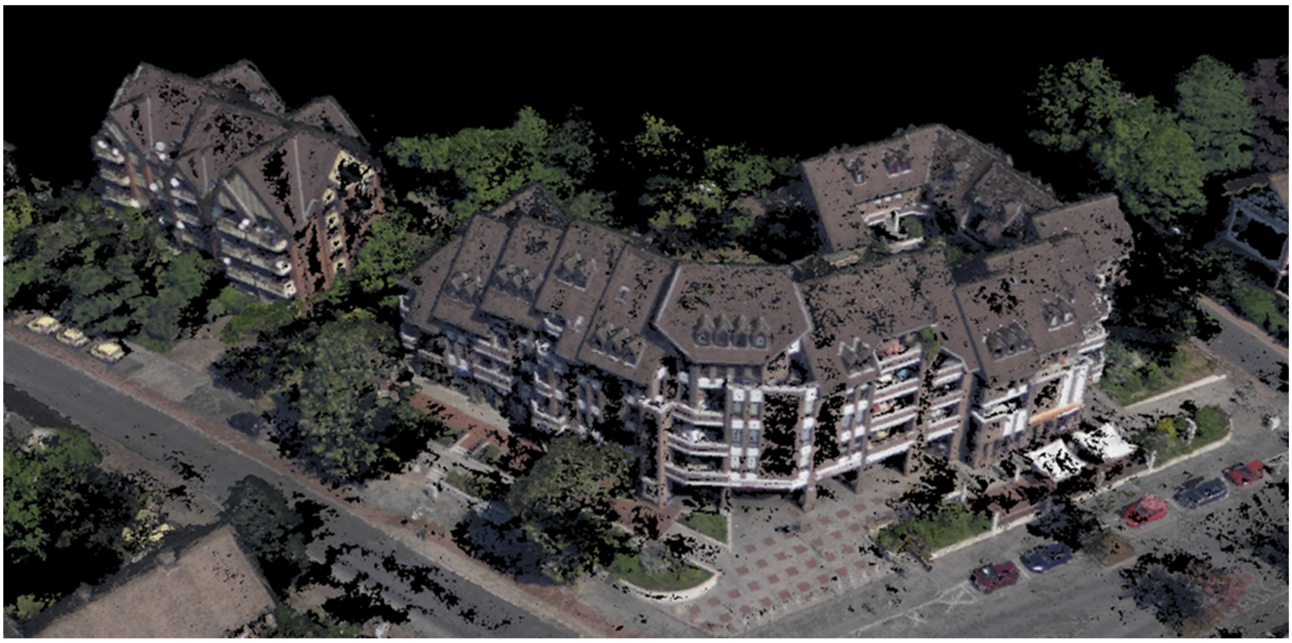

Figure 14: Reconstructed houses, 3D structure of balconies, cars and gable can be obtained.

### 3.3. Assessment Test of the VisionMap A3 System

As outlines before, the Institute for Photogrammetry conducted a second study concerning the capability of processing imagery collected by the oblique camera system A3 of VisionMap. For traditional nadir configurations vertical surfaces, as house facades, are occluded or only sparsely collected in the imagery. Obviously reconstructions of these areas are hindered. The A3 system overcomes this limitation collecting additional oblique imagery by stepping the sensor cross-flight during image collection. The collected imagery possesses largely varying viewing directions. As a result the appearance of world objects across the images differs and dense matching gets more challenging. The key concern within the study was how well the implemented matching and triangulation algorithms adapt to the advanced image configurations and radiometric properties in terms of reconstruction completeness and precision.

For the test Vision Map provided an oriented image block including city areas, vegetation and sea. Thereby a flight scenario with eight cameras mounted to an airplane was simulated. Each of the cameras was mounted at a certain angle increasing the obliqueness of collected imagery. Figure 15 displays the resultant image footprints on the ground.

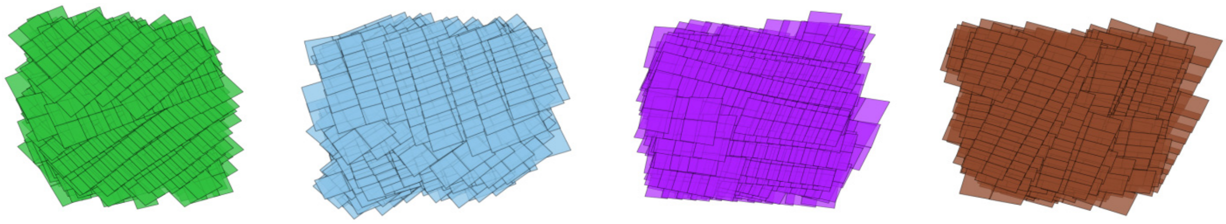

Figure 15: Footprints of the A3 imagery used within the test.

#### 3.3.1. Results of Stereo Matching and Triangulation

Within the test the achievable point density and accuracy was of special interest. Therefore the 41 slave images (Figure d) were matched against a common master image and triangulated using the multi-view correspondence linking implemented within SURE. To evaluate density on most challenging configurations, the selected master image provides a rather oblique viewing direction. The selection of the slave images was derived by an overlap analysis of the image footprints on the ground.

The completeness and precision of matching heavily depends on the similarity of image content between the master (base) and the slave images. This similarity can be estimated by the angle $\alpha$ of the two rays connecting a reconstructed object point and the optical centers of master and slave images. Since these angles are varying for each pair of corresponding pixels, the average of all angles from successfully extracted correspondences across a stereo pair is calculated. This angle will be denoted as $\alpha_{mean}$ and will be the reference unit in the further evaluations. Within the test six sub sets of stereo models were fused and compared. The stereo models contained by each subset were selected based on the average ray intersection angle $\alpha_{mean}$. The sets were defined by all models possessing an $\alpha_{mean}$ smaller than some defined threshold. The thresholds were chosen to be 5°, 10°, 15°, 20°, 25° and 35°. Disparity maps of the single subsets were fused (resulting in one point cloud) and precision was examined. Latter is expressed as standard deviations of depth estimations as available from the covariance matrices in the triangulation step. Since standard deviations $\sigma^i_D$ for the i single triangulated points are varying, $\sigma^i_D$ of all successfully reconstructed points were averaged and denoted as $\sigma_D^{mean}$. All numeric results as well as the number of models are depicted in

Figure 16. Obviously for an increasing number of incorporated models precision of points improves due to better ray intersection angles and larger number of rays used for the triangulation of single points. Fusion of 41 proximate depth maps results in depth accuracy of $\sigma_O^{mean} = 4.09$cm and 90.5% successfully matched pixels. However, processing time could be reduced from 21.5min to 15.0 minutes if only stereo pairs providing a $\alpha_{mean} < 20^o$ would be selected. For this configuration depth precision evaluates to 5.5cm and completeness amounts 87.78%. Despite the comparable large surface to camera distances, the signal-to-noise ratio seems to be in a range which does not negatively influence the dense matching process.

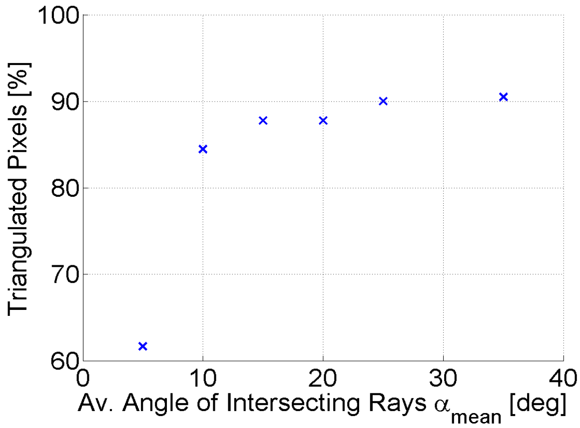


(a): Percentage of sucesfully computed pixels in the master image for the six subsets of stereo models

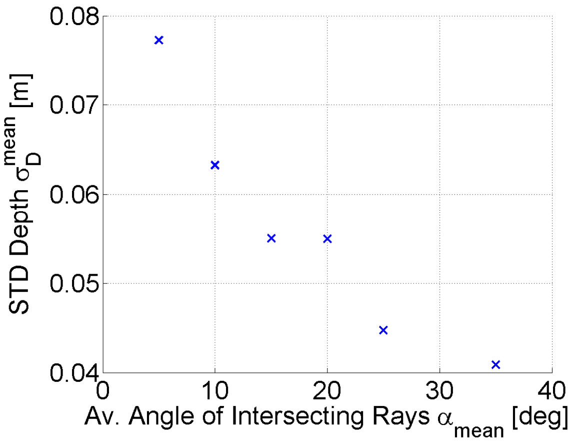


(b): Mean standard deviations of estimated depths for the six subsets of stereo models

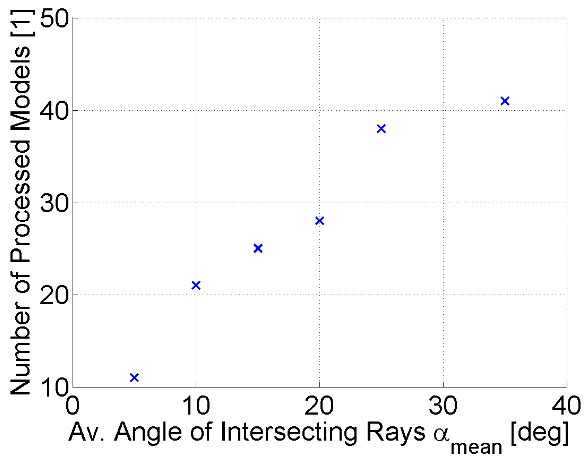


(c): Number of stereo models incooporated in the six subsets of stereo models

(d):Visualization of all slave images used within the test

Figure 16: Charts of numerical results.

The reconstruction quality heavily depends on local image texture and geometric properties of the surface. For the visualization in Figure 17 the standard deviation of depth estimates for each individually reconstructed point was assigned to its X, Y, Z coordinates. Thereby accuracies are decoded by the color. Dark blue represents a $\sigma^i_D$ of 1cm, red represents standard deviations equal and larger than 20cm. For low textured parts, as streets and house facades, $\sigma^i_D$ are generally larger than in well textured parts. Moreover, for facades points a reduced number of redundant disparity estimations leads to lower precision. The reconstruction of vegetation as trees o bushes is challenging since for different viewing angles their appearance heavily changes. Best results are obtained for rather planar surfaces providing good texture as the dirt road in the current example.

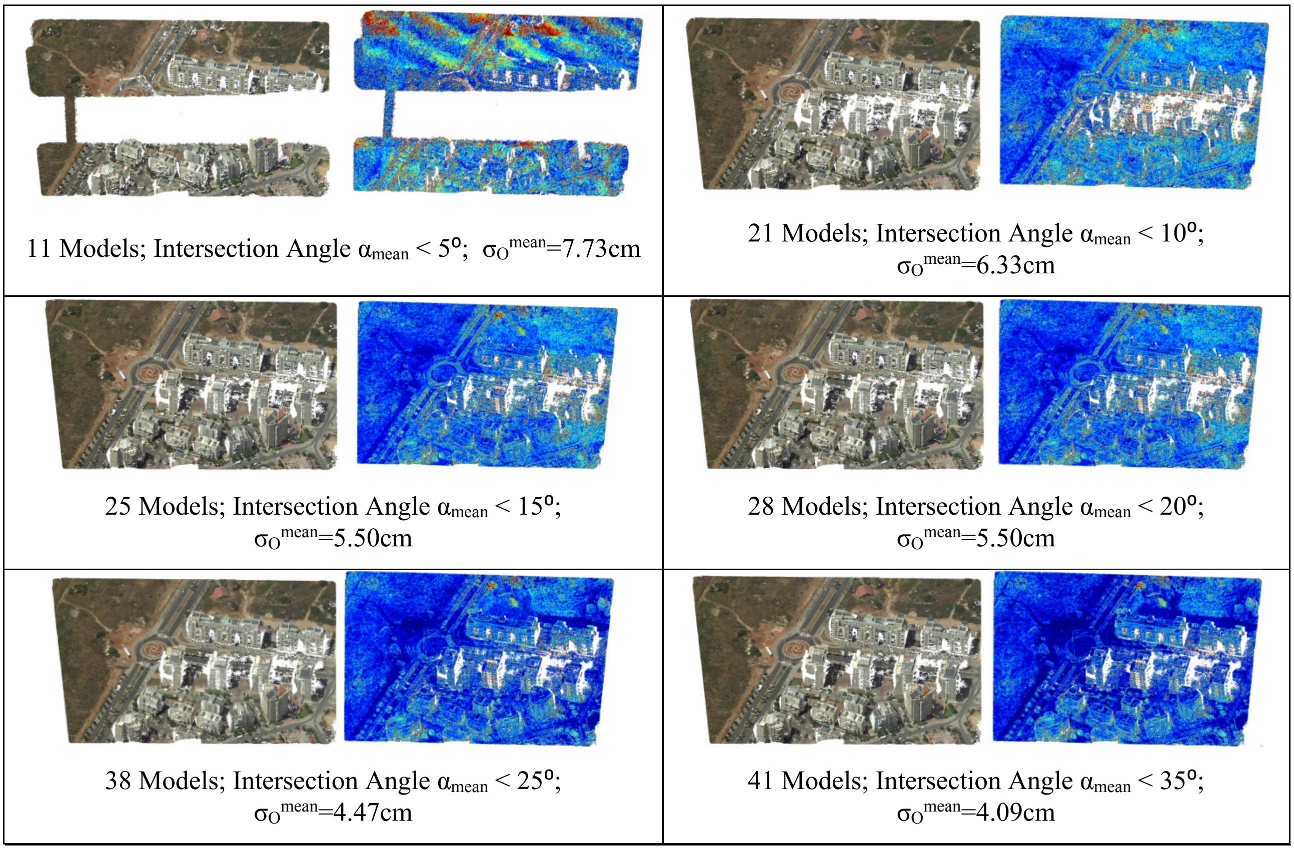


Figure 17: RGB point clouds and respective representation of per-depth standard deviations. Dark blue represents a $\sigma^i_D$ of 1cm, red represents standard deviations equal and larger than 20cm.

### 3.3.2. Processing Larger Areas – Completeness Evaluation

In the previous section a single oblique master image was matched against its 41 slave images and results were fused. For the latter exemplary oblique view facades could be reconstructed in large parts. Since the scene structure and block configuration is not completely homogenous, results from the previous test might not be representative for all parts of a larger surface. Moreover, clouds of proximate master images do spatially overlap. Particularly surfaces occluded in one master image might be seen in neighboring images and fusion of the respective point clouds might further increase the completeness of the reconstruction. Within this section the achievable completeness of the reconstruction for a larger test area was investigated. Therefore 7782 disparity maps were generated and triangulated. This resulted in 354 point clouds (~52 Gigabyte binary *.las format). In the central part of the selected area the surface could be reconstructed rather complete. As displayed in figure 18 even small structures like thin bars on top of the buildings or cars could be extracted clearly.

A general problem for dense image matching is shadowed surface areas. Due to reduced radiometric resolution matching fails more often which leads to higher local noise levels and decreased density in the final depth estimations. Moreover a larger number of image pairs were processed and processing time for matching amounted up to 111.25 hours. Time for point triangulation amounted to 20.6h (i7, 3.4GHz, 4cores). Whereas only few redundant measurements are available on the facades, ground points are collected with high redundancy. Therefore, the selection of incorporated stereo pairs certainly can be improved, leading to a reduced number of models at a comparable density of surface points. Point clouds are colored with respect to their correspondent master images. In the present data set we found large variances in radiometry in the imagery. Simply merging the point clouds in object space without any color adaption make the final point clouds look blurry or stained. Therefore our next step will be the implementation of an efficient approach for the fusion of high quality depth maps handling geometry as well as color information in a suitable way.

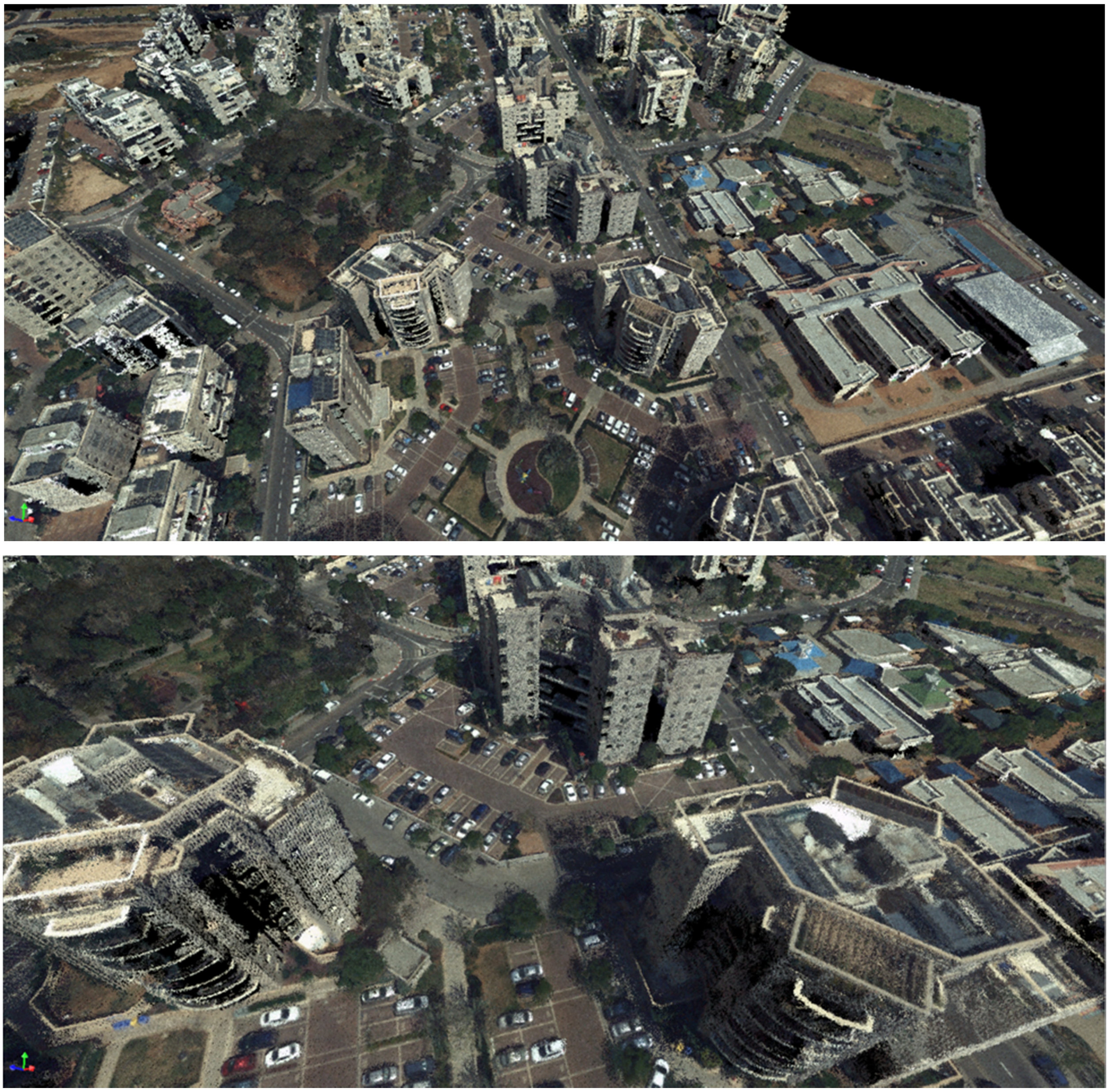

Figure 18: Detailed visualizations of the generated point clouds.

## 4. RECOMMENDATIONS

The processing of digital airborne nadir and oblique imagery using dense image matching algorithms – as implemented in SURE, the software of the Institute for Photogrammetry, University of Stuttgart – delivered some details to be shared in this paper.

1. In order to get as much as possible multi-view stereo configurations the inflight overlap should be at least 75%, what is not difficult to realize.
2. Best results for precise and complete 3D point clouds have been obtained with cross overlaps of more than 60%, which is contradictory to current NMCA flight patterns of up to 30%. Further tests with the new PentaView systems should be made to get those flight patterns suitable for the tasks to be solved in 3D city modeling and 3D corridor mapping.
3. As DIM algorithms require precise knowledge of the exterior orientation parameters of the individual images integrated sensor orientations (ISO) can play a crucial role for penta-view imagery. The tilting angles of the oblique cones are known and can be used as additional information to derive the corresponding orientation angles.
4. In-situ camera calibration is an essential task also for PentaView systems. The old set of Ebner (12) and Gruen (44) parameters should be substituted by the new developments in camera self-calibration to provide additional parameters well-suited for digital airborne camera systems (R. Tang et al., 2012a, b). Here, either Legendre or Fourier additional parameters will provide the basis to improve precision and to model remaining error sources efficiently in an extended bundle block adjustment.

## 5. CONCLUSIONS

Using digital oblique aerial camera systems will considerably extent the mapping spectrum of airborne photography. Combining nadir and oblique views simultaneously provide point clouds of high accuracy and completeness for highly modulated terrain and digital surface models, which represent the necessary data sources for 3D building reconstructions. First studies have shown, that an extension of automated approaches for 3D city modeling seems to be feasible. Therefore, the task to detect and reconstruct automatically unregistered buildings in 3D should not be a dream anymore.

This paper has introduced two test scenarios for using dense image matching to process airborne nadir and oblique imagery in one step. Both studies delivered successful results. The Luenen imagery – although collected at two different time epochs – could be processed finally as one large image block containing both views. The only problem here to overcome was the exact location and orientation of the oblique image shots, which was provided by the BINGO bundle block adjustment. With the new PentaView systems this will no more be a problem at all. In addition, the GNSS/IMU direct sensor orientation will deliver the exterior orientation parameters needed to start with the DIM processing.

The DIM processing of the A3 stepping frame camera geometry delivered point clouds of high geometric accuracy. Even small thin structures of GSD resolution could be reconstructed. The overall completeness of the matched pixels could be measured close to 90%. Despite the comparable large surface to camera distances, the signal-to-noise ratio seems to be in a range which does not negatively influence the dense matching process.

Oblique aerial camera systems are in line with the evolution of digital nadir camera systems for aerial photography. The existing solutions for integrated sensor orientations, bundle block adjustments and dense image matching can be used without any difficulties. It will be interesting to see the extensions of 3D city modeling and corridor mapping – besides the classical product portfolio showcasing also some impact of those new aerial imaging systems. The idea of "All-In-One Photogrammery" will come true.

## 6. ACKNOWLEDGEMENTS

The Institute for Photogrammetry, University of Stuttgart is cooperating about two decades with vendors of photogrammetric data collection systems. Needless to say, that the Vaihingen/Enz testsite is continuously used for performance tests of GNSS/IMU integrations and to validate camera geometries.

The long-time cooperation with IGI mbH, Kreuztal, Germany, in this respect is gratefully acknowledged. Thanks also to AEROWEST GmbH Dortmund for offering the Luenen aerial photography for combining nadir and oblique imagery for the DIM performance study test.

The close cooperation with VisionMap, Tel Aviv, Israel for the last three years is also highly appreciated. The results of the geometric performance of the A3 system and 3D point cloud processing using SURE have given new insights into the stepping frame camera concept.

## 7. REFERENCES

Books and Journals:

Brenner, C. (2001): City Models – Automation in Research and Practice. In: Photogrammetric Week '01, Eds. D. Fritsch & R. Spiller, Wichmann, Heidelberg, pp. 149-158.

Fritsch, D. (1997): Experiences with the Airborne Three-Line Camera System DPA. In: Photogrammetric Week '97, Eds. D. Fritsch & D. Hobbie, Wichmann, Heidelberg, pp. 63-74.

Fritsch, D., Grimm, A., Kremer, J. (2012): Towards All-in-One Photogrammetry. GIM International, Feature, April 2012, pp. 18-23.

Fritsch, D., Grimm, A., Kremer, J., Rothermel, M., Wenzel, K. (2013): Bilddatenerfassung mit einem Gyrocopter – Erste Erfahrungen zur „Photogrammetrie nach Bedarf". DGPF Tagungsband 22/2013, Dreiländertagung, Freiburg.

Gruber, M., Walcher, W. (2013): Oblique Image Collection – Challenges and Solutions. In: Photogrammetric Week '13, Ed. D. Fritsch, Wichmann, Berlin and Offenbach, pp. 111-115.

Hirschmüller, H. (2005): Accurate and Efficient Stereo Processing by Semi Global Matching and Mutual Information. IEEE Conference for Computer Vision and Pattern Recognition, 2, pp. 807-814. San Diego, CA, USA.

Kada, M. (2009): The 3D Berlin Project. In: Photogrammetric Week '09, Ed. D. Fritsch, Wichmann, Heidelberg, pp. 331-340.

Karbo, N., Schroth, R. (2009): Oblique Aerial Photography: A Status Review. In: Photogrammetric Week '09, Ed. D. Fritsch, Wichmann, Heidelberg, pp. 119-125.

Petrie, G. (2009): Systematic Oblique Aerial Photography Using Multiple Digital Cameras, Photogrammetric Engineering & Remote Sensing (PERS), pp. 102-107.

Raizman, Y. (2013): High Troughput Aerial Photography, Ortho & 3D Processing. In: Photogrammetric Week '13, Ed. D. Fritsch, Wichmann, Berlin and Offenbach, pp. 101-109.

Rothermel, M., Wenzel, K., Fritsch, D., Haala, N. (2012): SURE: Photogrammetric Surface Reconstruction from Imagery. Proceedings LC3D Workshop, Berlin, December 2012.

Talley, B. B., (1938): Multiple lens aerial cameras, Chapter IV in Aerial and Terrestrial Photogrammetry, pp. 91-116, Pitman Publishing Corporation, New York & Chicago.

Tang, R., Fritsch, D., Cramer, M., Schneider, W. (2012a): A Flexible Mathematical Method for Camera Calibration in Digital Aerial Photogrammetry. Photogrammetric Engineering & Remote Sensing (PERS), Vol. 78, pp. 1069-1077.

Tang, R., Fritsch, D., Cramer, M. (2012b): New Rigorous and Flexible Fourier Self-Calibration Parameters for Airborne Camera Calibration. ISPRS Journal of Photogrammetry and Remote Sensing, 71, pp. 76-85.

Wagner, R. (2013): Urban Mapping Applications. In: Photogrammetric Week '13, Ed. D. Fritsch, Wichmann, Berlin and Offenbach, pp. 89-99.

Wenzel, K., Rothermel, M., Haala, N., Fritsch, D. (2013): SURE – The ifp Software for Dense Image Matching. In: Photogrammetric Week '13, Ed. D. Fritsch, Wichmann, Berlin and Offenbach, pp. 59-70.

www:
http://en.wikipedia.org
http://www.ifp.uni-stuttgart.de/publications/phowo.en.html